

May 30th, 10:45 AM - 11:00 AM

Investigation of the Flow Field inside a Drainage System: Gully - Pipe - Manhole

N. A. Beg
University of Coimbra

R. F. Carvalho
University of Coimbra

J. Leandro
University of Coimbra

P. Lopes
University of Coimbra

L. Cartaxo
University of Coimbra

Follow this and additional works at: <http://digitalcommons.usu.edu/ewhs>

 Part of the [Civil and Environmental Engineering Commons](#)

Beg, N. A.; Carvalho, R. F.; Leandro, J.; Lopes, P.; and Cartaxo, L., "Investigation of the Flow Field inside a Drainage System: Gully - Pipe - Manhole" (2016). *International Junior Researcher and Engineer Workshop on Hydraulic Structures*. 4.
<http://digitalcommons.usu.edu/ewhs/2016/Session1/4>

This Event is brought to you for free and open access by the Conferences and Events at DigitalCommons@USU. It has been accepted for inclusion in International Junior Researcher and Engineer Workshop on Hydraulic Structures by an authorized administrator of DigitalCommons@USU. For more information, please contact dylan.burns@usu.edu.



Investigation of the Flow Field inside a Drainage System: Gully – Pipe – Manhole

Md N. A. Beg¹, R. F. Carvalho¹, J. Leandro¹, P. Lopes¹ and L. Cartaxo¹

¹MARE - Marine and environmental research center
Department of Civil Engineering, University of Coimbra,
Coimbra, Portugal
E-mail: mnabeg@uc.pt

ABSTRACT

Gully drop connected with manhole is one crucial structural part in several urban drainage systems. This paper analyses the flow pattern and flow hydraulics of a gully-manhole drainage structure. Analysis is done numerically using computational fluid dynamics CFD tools OpenFOAM®. Data from the Dual Drainage / Multi Link Element installation (DD-MLE) at the University of Coimbra hydraulic lab is used to validate the numerical simulations. The experimental model setup consists of a 0.5 m wide channel, a $0.6 \times 0.24 \times 0.32$ m ($L \times W \times D$) gully, a gully outlet with an 80 mm diameter pipe and a manhole of 1 m diameter with a 300 mm inlet and outlet pipe connected. The flow pattern is observed under drainage flow conditions with different surcharge heights of the manhole. It has been observed that the intercepted flow through the gully decreases with the increase of surcharge in the manhole. The shear stress at the gully floor is found much higher than that of manhole floor. This indicates the probability that bigger sediment particle can be transported through gully but will remain deposited at the manhole floor. The flow pattern in the manhole changes with the change of surcharge height. The flow through the manhole inlet seems to disperse less at higher surcharge.

Keywords: Computational Fluid Dynamics (CFD), Urban drainage, OpenFOAM®, Gully-Manhole

1. INTRODUCTION

Urban flooding is one of the biggest issues for a large city. Predicting urban drainage flows accurately is an important way in preventing or minimizing flood risks. In most cities, urban drainage system is the only pathway to convey the flood water from urban areas. The system is usually described as two different sets of components; the major system or overland system is composed of surface paths and temporary storage areas and the minor system or below ground system is composed of pipes and manholes. Gullies work as the connectors between the two systems. They collect the runoff from paved and unpaved system and supply manholes. During a high flood event, pressurized flow may occur and create back flow from the manhole to the surface (Butler and Davies 2011; Djordjević et al. 2013; Lopes et al. 2015). To assess the flood risk in a city, evaluation of the drainage efficiency of a gully is necessary.

Some works have been done by different authors to characterize individually gully and manhole hydraulics. Galambos (2012) used ANSYS Fluent CFD tools to validate 3D and 2D/3D CFD models and a number of computational simulations on different gratings. His works also extended to better understand the effect of various geometric and road alignment on the intercepted flow. Lopes et al. (2016) used three dimensional model with VOF surface capturing technique using OpenFOAM® to analyse gully efficiency with the grate's slots aligned in the flow direction and compared with experimental data sets. Djordjević et al. (2013), Martins et al. (2014) and Leandro et al. (2014) presented both experimental and numerical investigation for drainage condition of a gully. On the other hand, Lopes et al. (2015) showed analysis of the flow field in a gully with surcharge condition. Romagnoli et al. (2013) measured the turbulence characteristics of gully for reverse flow. Several works have been done on manhole as well. Stovin et al. (2008) have showed a number of possible methods to validate CFD model, while Rubinato (2015) has showed uses of scaled models to quantify hydraulic losses in a manhole. Beg et al. (2016) used OpenFOAM® with VOF model to assess flow path line and manhole pressure variation in surcharged manhole and compared with experimental results.

In this work, both gully and manhole hydraulics were analysed together using three dimensional CFD model OpenFOAM®. The geometry of the numerical model was a replication of a real scale dual drainage experimental model setup installed at the hydraulic laboratory of University of Coimbra. The work focuses on

different hydraulic properties on of the gully-manhole structure while draining to a surcharged manhole. These results may be used to aid the simulation of pollutant transport model in the drainage system.

This paper starts presenting the experimental and numerical modelling methodologies in section 2, followed by presenting the comparison between the numerical and experimental results and some analysis using the numerical model results in section 3. Conclusion is made in section 4.

2. METHODOLOGY

2.1. Experimental Setup

The experimental facility installed at the hydraulic lab of University of Coimbra was used for this study. A detailed description of the facility can be found at Carvalho et al. (2013). The facility contains a quasi-real scale multi-link dual drainage network to observe different phenomena of an Urban Drainage Network. For the current study, a part of the setup was used, containing a rectangular surface drain (0.5 m wide), a rectangular gully pot (0.6 m × 0.24 m × 0.32 m) and a circular manhole (1 m diameter) (Figure 1). The surface drain has a slope of 1:1000. The manhole is connected with 300 mm diameter inlet and outlet pipes and does not have any guide channel inside. The inlet-outlet pipes are parallel to the surface and has no slope. The gully is connected to the manhole with an angular pipe of 80 mm diameter, at an angle of 63° in plan and 90° in vertical. The manhole did not have any inflow from its top, however no lid was loosely placed at its top ensuring equal pressure at both sides. A discharge flow meter is installed at the end of the pipe and that is represented by a small contraction in the numerical model. The gully-manhole size and the slope replicate a typical drainage system in Portugal. But the size of the gully outlet pipe is smaller that of the design recommendation. The Portuguese legislation recommends a 200 mm pipe for the gully outlet which drains a flow of 100 l/s approximately. This was exchanged for an 80 mm pipe due to different limitations of experimental model setup installed.

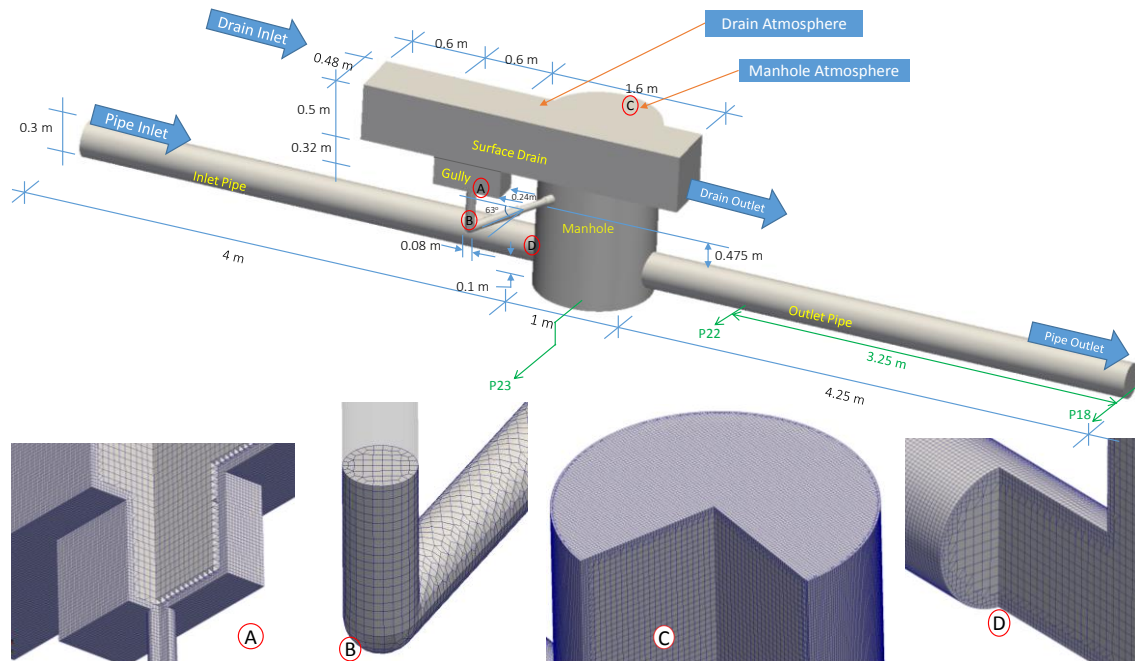


Figure 1: Upper Panel: Experimental setup; Lower panel: Computational mesh of different parts of the domain
A: Gully with outlet pipe, B: Outlet Pipe, C: Manhole and D: Pipe connected with Manhole

The system is equipped with three electromagnetic flow meters (not shown in the figure). The first one is located at the drain inlet, the second one is the referred at the pipe between manhole and gully and the third is at the outlet pipe; from which different discharge at the drain, gully and manhole can be measured.

Two separate experimental study data have been used for the numerical simulation. In the first experimental work, only the manhole with inlet and outlet pipe were used; in which a flow of 43.7 l/s was applied through the

manhole inlet (SE1). The second set of experimental works, flow through the drain and gully was observed; in which 19.8 l/s flow was measured upstream of the drain inlet (SE2). The grate of the gully was removed. The flow through the rectangular drain was an open channel flow with a flow depth of 8 cm in the channel; which yielded a Froude number of 0.6. Some part of the incoming drain inlet flow passed through the gully outlet to the manhole and the rest overflowed through the gully and made a free fall to the reservoir tank through the drain outlet. As the discharge was overflowing the gully top, the location of the water surface was located in the drain above the gully. The intercepted flow by gully enters the manhole as a free fall plunging jet with a recirculation zone in the manhole. This flow accumulates with the inflow through manhole inlet and flows out through the manhole outlet. The gully was given special attention. The velocity field at the gully was measured at three vertical planes using ADV (Acoustic Doppler Velocimetry). The first and the third planes are at 5 cm distance from the two longitudinal walls of the gully; which made each of the plans 7 cm apart from the central line of the gully. The second plane is the central plane. Each plane had 121 point measurements, at an interval of 4.8 cm and 2.5 cm towards horizontal and vertical directions respectively (Figure 2). The velocity measurement was taken inside the gully only and was not extended to the water surface.

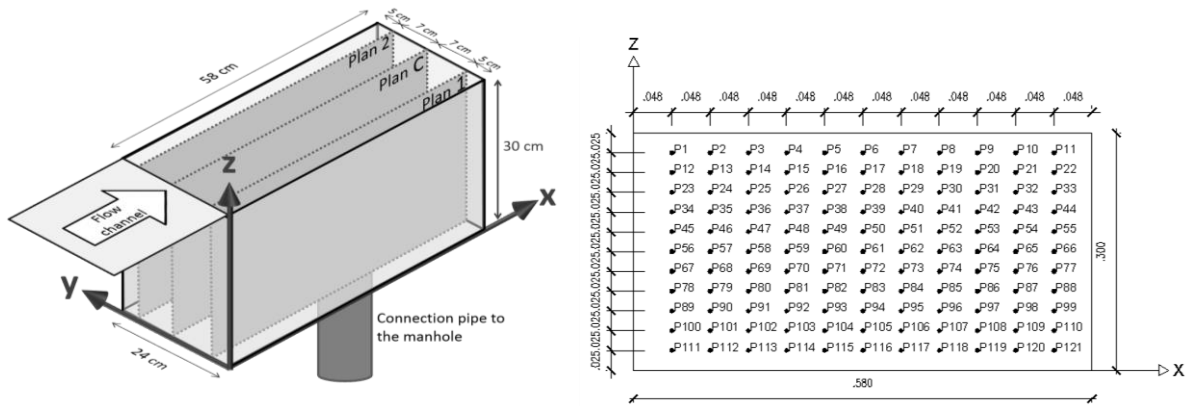


Figure 2: Velocity measurement locations using ADV. Left panel shows the location of the three planes and the right panel shows the point measurement locations at each plane

In the both experimental scenarios, the manhole was at surcharged condition and the manhole inlet-outlet pipe was pressurized. The surcharge height at the manhole was 0.67 m; which was 20.5 cm below the invert level of the gully outlet to the manhole.

2.2. Numerical Model Description

The objective of the numerical modelling is to characterize the incoming flow through the gully and check the flow path in the manhole during drainage condition. Open source three dimensional CFD model tools OpenFOAM® version 2.3.0 is used in this study. The solver *interFoam* is chosen which includes Volume of Fluid (VOF) method (Hirt and Nichols 1981) to track the free surface or interface location between two fluids. This method uses volume fraction indicator function α to determine the amount of liquid present in each cell. In case of $\alpha=0$ or 1, the cell volume is considered filled with air or water respectively; while $0<\alpha<1$ represents that the cell contains the free surface as it is partially filled with water.

The *interFoam* solver uses a single set of Navier-Stokes equations for the two fluids, water and air, and additional equations to describe free-surface where the velocity at free-surface is shared by both phases. The solver considers a system of isothermal, incompressible and immiscible two-phase flow. The model deals with Reynolds averaged conservation of mass and momentum,

$$\nabla \cdot \mathbf{u} = 0 \quad (1)$$

$$\frac{\partial \rho \mathbf{u}}{\partial t} + \nabla \cdot (\rho \mathbf{u} \mathbf{u}) = -\nabla p^* + \nabla \cdot \boldsymbol{\tau} + \mathbf{g} \cdot \mathbf{x} \nabla \rho + \mathbf{f}_\sigma \quad (2)$$

where \mathbf{g} is the acceleration due to gravity, \mathbf{u} is the velocity vector in the Cartesian coordinate, $\boldsymbol{\tau}$ is the shear stress tensor, p^* is the modified pressure adopted by removing the hydrostatic pressure ($\rho \mathbf{g} \cdot \mathbf{x}$) from the total pressure and \mathbf{f}_σ is the volumetric surface tension force.

The viscous stress term is defined by the incompressible Newton's law,

$$\nabla \cdot \boldsymbol{\tau} = \nabla(\mu(\nabla \mathbf{u})) + (\nabla \mathbf{u}) \cdot \nabla \mu \quad (3)$$

The advection equation to describe free-surface in VOF method (Hirt and Nichols 1981), which uses an interfacial compressive term to keep the interface region confined in a small space (Rusche 2002; Weller 2002) is described as:

$$\frac{\partial \alpha}{\partial t} + \nabla \cdot (\alpha \mathbf{u}) + \nabla \cdot [\mathbf{u}_c \alpha (1 - \alpha)] = 0 \quad (4)$$

The last term of equation (4) is the compressive term. The term $\alpha(1-\alpha)$ ensures that the compressive term or compressive velocity \mathbf{u}_c is calculated only at the interphase (when $0 < \alpha < 1$). This velocity acts at the perpendicular direction to the interface and defined as:

$$\mathbf{u}_c = C_\alpha |\mathbf{u}_c| \frac{\nabla \alpha}{|\nabla \alpha|} \quad (5)$$

C_α is a Boolean term (value is 0 or 1) which activates ($C_\alpha = 1$) or deactivates ($C_\alpha = 0$) the interface compressive term. The volumetric surface tension \mathbf{f}_σ is calculated by the Continuum Surface Force model (Brackbill et al. 1992).

$$\mathbf{f}_\sigma \approx \sigma \kappa \nabla \alpha \quad (6)$$

Here, κ is referred as the surface curvature.

To model the turbulence phenomena, $k-\varepsilon$ turbulent modelling approach is used. This turbulence calculation approach uses two closure equations for k (*turbulent kinetic energy*) and ε (Energy dissipation). The unsteadiness in flow is averaged out in this model and regarded as part of the turbulence (Furbo et al. 2009).

The value of k is calculated along with ε using $k-\varepsilon$ turbulent model. The dynamic viscosity (μ) is calculated as:

$$\mu = \rho(v_t + v_0) \quad (7)$$

where, v_0 and v_t are molecular viscosity and turbulent viscosity respectively.

2.3. Mesh Generation

Mesh generation is one of the most important issue in CFD modelling. The quality of mesh is the key to have quality result from the model. The construction of the computational mesh for this study, was done as follows: (1) the geometry was prepared using open source software SALOME v.7.5.1; (2) the geometry was exported to Stereolithography (STL) format. (3) another open source meshing tool *cfMesh* (Juretić 2015) was used to prepare the mesh. This tool prepares three dimensional hexahedral mesh in the Cartesian planes. The maximum mesh size is kept as 2 cm towards all the three directions. The mesh was further refined at the walls and joins of different geometrical shapes. The created computational mesh has 821,500 computational cells with a little more than 1.01 million nodes. Some of the mesh properties can be seen at Figure 1 and Table 1.

Table 1: Quality parameters of the computational mesh

| Parameter Name | Max. Aspect ratio | Max. skewness | Max. non-orthogonality | Avg. non-orthogonality | Min. face area (m ²) | Max. face area (m ²) | Min. volume (m ³) | Max. volume (m ³) |
|----------------|-------------------|---------------|------------------------|------------------------|----------------------------------|----------------------------------|-------------------------------|-------------------------------|
| Value | 7.27 | 1.708 | 51.32 | 4.13 | 3.45x10 ⁻⁰⁶ | 4.72x10 ⁻⁰⁴ | 4.19x10 ⁻⁰⁹ | 1.06x10 ⁻⁰⁵ |

2.4. Boundary conditions

Six open boundaries were used for the computational domain. They are: Drain Inlet, Drain Atmosphere, Drain Outlet, Pipe Inlet, Pipe Atmosphere and Pipe Outlet. The drain inlet was further divided in to two parts for the incoming water and air phases respectively. The boundary data are calculated from the experimental model

completed before. The upstream boundaries were obtained from measured discharge data while the downstream pressure data were obtained from observed water depths in the drain and manhole.

As the simulation used $k-\varepsilon$ turbulent approach, OpenFOAM® requires six types of Boundary Conditions (BC) for each boundary. They are *alpha.water* (water volume fraction in each cell), \mathbf{u} (velocity vector in Cartesian domain), *p_rgh* (relative bottom pressure corresponding to datum), k (turbulent kinetic energy), ε (energy dissipation) and *nut* (turbulent viscosity). The first three BC's are required for hydraulic modelling while the last three are required for turbulence calculation.

For both inlets, fixed velocity/discharge were applied using *alpha.water* and U . Pressure data (*p_rgh*) were prescribed at the outlet boundaries. Both of the atmosphere boundaries were kept as *zeroGradient* velocity and relative air pressure as zero; so that air could be exchanged if needed. All the wall BC's were kept as no-slip condition (i.e. velocity = 0). For the turbulent approach, values of k , ε and *nut* were calculated using the equations in FLUENT manual (ANSYS Ins 2009), considering medium turbulence at the gully and manhole. All the walls are prescribed as *wallFunction* as this eliminates the necessity of fine layered boundary mesh and hence reduce the computational time (Greenshields 2015).

Three different numerical model setups were simulated using the same mesh. The setups are described in Table 2. The first scenario replicates the experimental setup while the second and the third scenarios use a higher surcharge level in the manhole, in a view of checking the change of flow condition in the gully due to the higher surcharge level in the manhole.

Table 2: Numerical model scenarios

| | Drain inlet Q (l/s) | Manhole inlet Q (l/s) | Manhole surcharge level (m) | Remarks |
|--------------|---------------------------------|-----------------------------------|--|---|
| Simulation 1 | 19.8 | 43.7 | 0.67 | Experimental case scenario = SE1 & SE2 |
| Simulation 2 | 19.8 | 43.7 | 1.16 | Additional scenario 1 |
| Simulation 3 | 19.8 | 43.7 | 1.47 | Additional scenario 2 |

2.5. Simulation of the models

The model was ready to run after the boundary setup. During the simulation, *adjustableRunTime* was used keeping maximum CFL number to 0.8. Cluster computing system at the University of Coimbra was used to run the simulations using MPI mode with 16 processors. Each simulation took 40 sec to reach steady state. The computation time was 138 hours for each simulation. Results were obtained once the simulation reached steady state.

3. RESULTS AND DISCUSSION

3.1. Comparison with experimental work at the gully

The numerical model results are compared with the experimental study data of the velocity profiles at the gully obtained by the Vectrino acoustic velocimetry. Figure 3 shows s contours at the three different planes and Figure 4 shows comparison of longitudinal and vertical velocity profiles at different location of the gully.

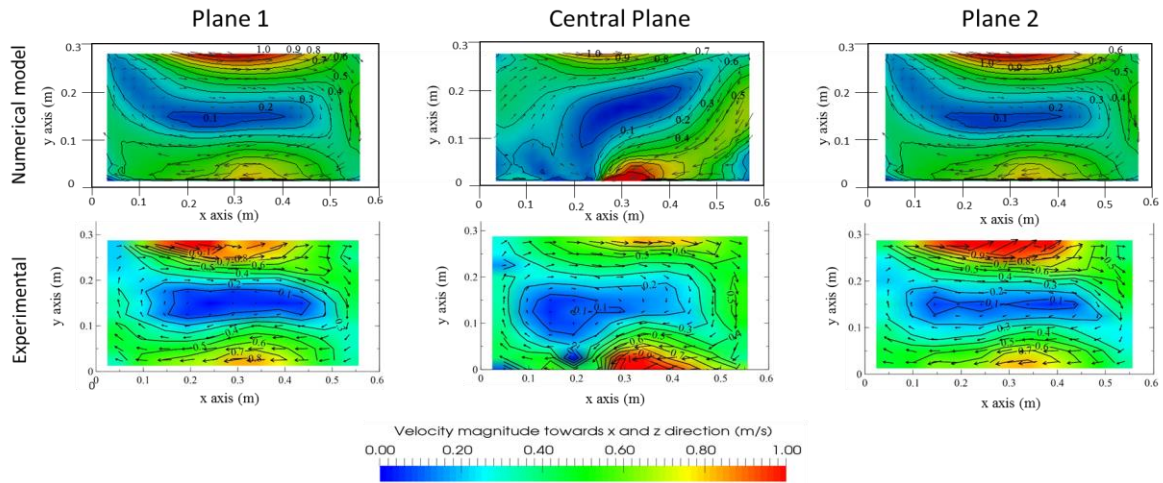


Figure 3: Comparison of velocity between numerical (upper panel) and experimental (bottom panel) study at three longitudinal planes of the gully

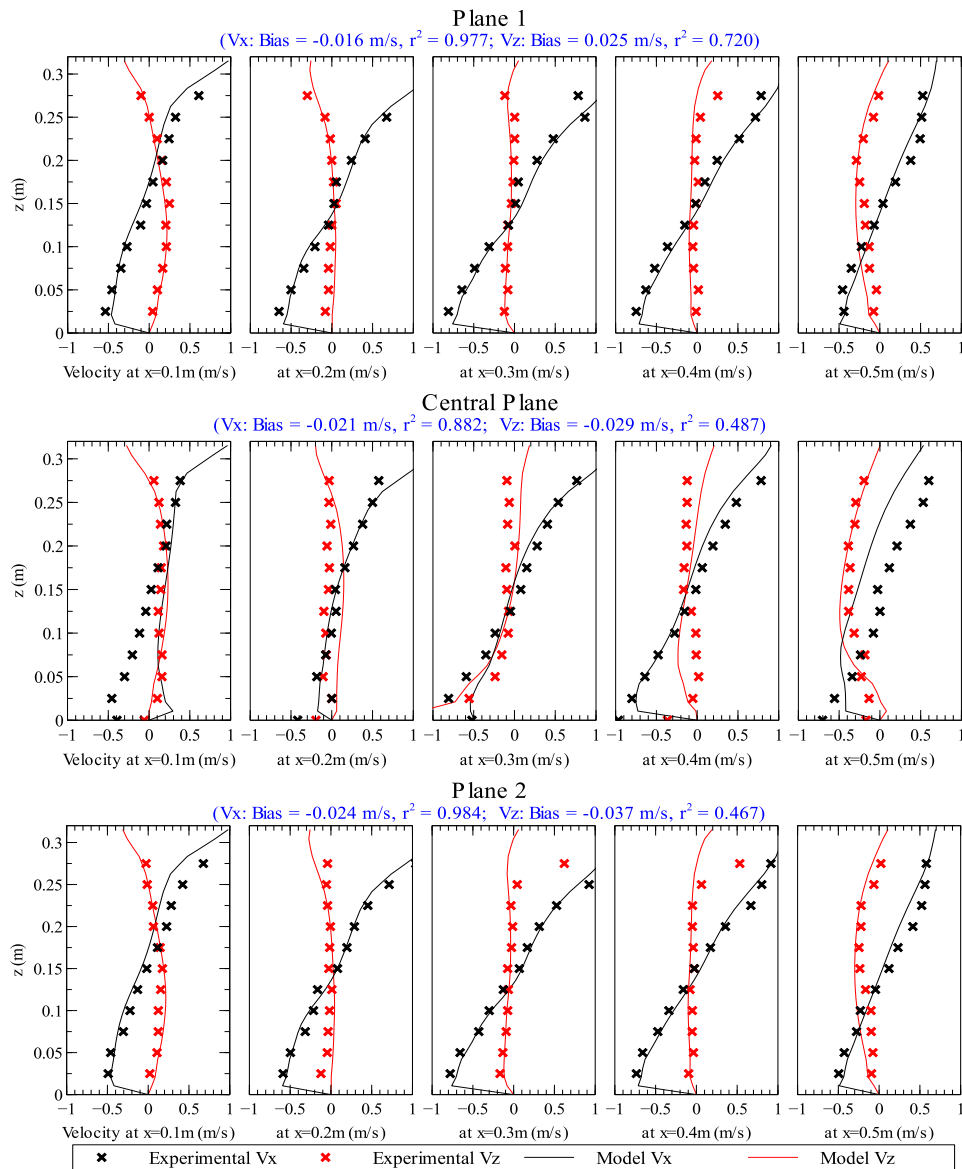


Figure 4: Velocity profile at different location of gully. Firm lines showing numerical model data and cross (x) markers showing data from experimental study

It can be seen from Figure 3 and Figure 4 that the numerical model shows good agreement with experimental data. The vertical vortex size and location created in the numerical result shows similarity to those observed in the experimental model data. Average statistical comparison between the two data can be shown in at Figure 4 and more detailed in Table 3. It shows that the model can reproduce the longitudinal velocity component (V_x) very well (average $r^2 = 0.95$ and BIAS = -0.004 m/s). The representation of vertical velocity component (V_z) in the gully is at satisfactory level (average BIAS 0.011 m/s and $r^2 = 0.56$).

Table 3: Statistical BIAS and correlation coefficient (r^2)

| | | BIAS | | | | | r^2 | | | | | | |
|-------------|-------|----------|----------|----------|----------|----------|---------------|----------|----------|----------|----------|----------|-------------|
| | | $x=0.1m$ | $x=0.2m$ | $x=0.3m$ | $x=0.4m$ | $x=0.5m$ | Avg. | $x=0.1m$ | $x=0.2m$ | $x=0.3m$ | $x=0.4m$ | $x=0.5m$ | Avg. |
| P 1 | V_x | 0.060 | 0.014 | -0.078 | -0.068 | -0.007 | -0.016 | 0.99 | 0.97 | 0.98 | 0.99 | 0.96 | 0.98 |
| P C | | -0.223 | -0.034 | -0.024 | -0.009 | 0.186 | -0.021 | 0.67 | 0.93 | 0.95 | 1.00 | 0.87 | 0.88 |
| P 2 | | 0.096 | 0.023 | -0.010 | -0.016 | 0.028 | 0.024 | 0.99 | 0.99 | 0.99 | 0.98 | 0.97 | 0.98 |
| Avg. | | -0.023 | 0.001 | -0.037 | -0.031 | 0.069 | -0.004 | 0.935 | 0.88 | 0.96 | 0.97 | 0.99 | 0.95 |
| P 1 | V_z | 0.004 | -0.031 | 0.009 | 0.072 | 0.073 | 0.025 | 0.87 | 0.70 | 0.53 | 0.79 | 0.71 | 0.72 |
| P C | | -0.020 | -0.141 | 0.015 | -0.020 | 0.021 | -0.029 | 0.36 | 0.05 | 0.84 | 0.53 | 0.65 | 0.49 |
| P 2 | | -0.029 | -0.021 | 0.069 | 0.079 | 0.089 | 0.037 | 0.85 | 0.05 | 0.02 | 0.71 | 0.71 | 0.47 |
| Avg. | | -0.015 | -0.064 | 0.031 | 0.044 | 0.061 | 0.011 | 0.69 | 0.27 | 0.46 | 0.68 | 0.69 | 0.56 |

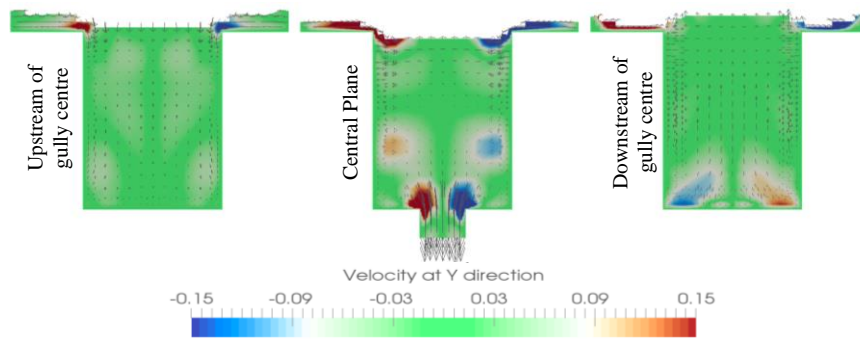


Figure 5: Transverse velocity (V_y) at the gully

Figure 5 shows the transverse velocity (V_y) in the gully at three different transects. It can be seen from Figure 5 that transverse velocity is very low, in the range of -3 cm/s to $+3$ cm/s. This velocity component was found insignificant to compare with experimental results.

3.2. Pressure and Shear stress

The pressure and the wall shear stress at the gully bottom were analyzed and can be seen in Figure 6. Similar plot have been made for the bottom of the manhole in Figure 7. In both of the figures, the water flows from the left to right.

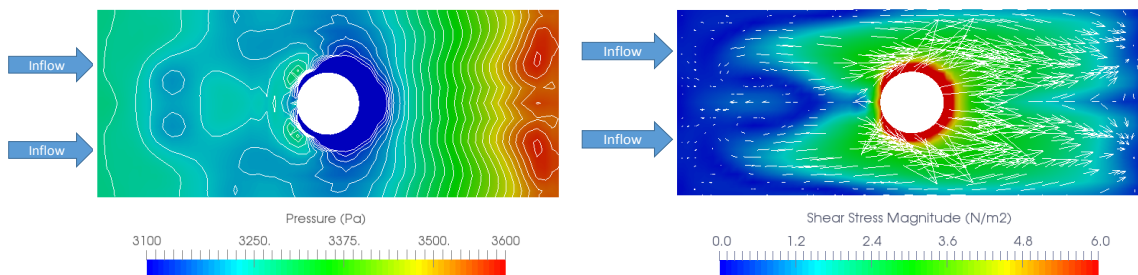


Figure 6: Pressure variation (left panel) and wall shear stress (right panel) at the bottom of the gully

It can be seen from Figure 6 that the bottom pressure at the gully is not uniform. Excluding the outlet location, the pressure gradually increases from upstream direction to the downstream direction. The deviation of the pressure at the gully bottom is in the range of 300 Pa. At the right panel of Figure 6, the wall shear stress at the gully bottom can be seen. The figure shows that the shear stress at the immediate upstream of the gully outlet is the highest. The shear stress direction can be seen towards the opposite direction of the flow.

From Figure 7, a similar view of bottom pressure and shear stress at the manhole bottom can be found. Like the gully bottom, the pressure at the manhole bottom also increases from the downstream to the upstream. Here the variation of bottom pressure is in the range of 200 Pa. The bottom shear stress shows higher value near the outlet. Both bottom shear stress and pressure diagram are asymmetric at the manhole bottom; whereas those diagrams showed symmetric pattern at the gully bottom. The influence of oblique flow from the gully outlet might be the reason of this asymmetric pattern.

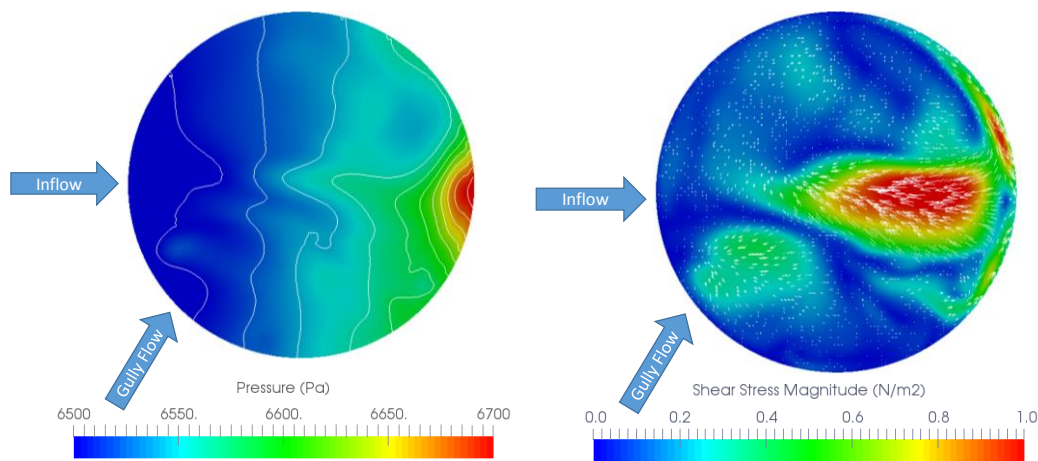


Figure 7: Pressure variation (left panel) and wall shear stress (right panel) at the bottom of the manhole

The pressure and shear stress diagrams at the bottom of the two structures might be useful in predicting sediment deposition pattern inside the structures. The pressure and shear stress diagrams at the bottom of the two structures might be useful in predicting sediment deposition pattern inside the structures. It is likely that in case of particulate transport in the system, the particles are more likely to be deposited at the region with higher pressure with lower shear stress and erosion may take place at the region with higher shear stress and lower pressure. A relation between critical shear stress and sediment particle size is given by Berenbrock and Tranmer (2008). The shear stresses at the gully bottom are in the range of 3 to 6 N/m². This stress is higher than the critical shear stress of fine gravel ($D_{50} = 4-8$ mm) While the shear stresses at the manhole bottom are in the range of 0.4 to 1.0 N/m², which is more than the critical shear stress of coarse sand ($D_{50} = 1$ to 2 mm). So it is likely that gully flow can transport sediment particles up to 8 mm; while the manhole flow can transport sediment particles of up to 2 mm. The bigger sediment particles are likely to be deposited at the manhole bottom.

3.3. Flow path line

During the experimental and numerical study, the following flow distribution (Table 4) was observed at different part of the domain.

Table 4: Flow distribution

| Simulation | Drain Inlet (l/s) | Drain Outlet (l/s) | Gully Pipe (l/s) | Manhole Pipe Inlet (l/s) | Manhole Pipe Outlet (l/s) |
|--------------|-------------------|--------------------|------------------|--------------------------|---------------------------|
| Simulation 1 | 19.80 | 12.4 | 7.4 | 43.7 | 51.1 |
| Simulation 2 | 19.80 | 13.4 | 6.4 | 43.7 | 50.1 |
| Simulation 3 | 19.80 | 15.9 | 3.9 | 43.7 | 47.6 |

In all the three simulations, the inflows at the drain inlet were 19.80 l/s. The intercepted flow by the gully was 7.4 l/s (40 % of the inflow) at the experimental case scenario (Simulation 1). The remaining 12.4 l/s (60 % of the inflow) was over flown through the drain. The discharge at the manhole outlet was 51.7 l/s of which 15 % was coming through the gully and the remaining 85 % was coming through the manhole inlet pipe. At simulation 2 and 3, with the increase in manhole surcharge, the flow through the gully outlet decreases. Out of 19.8 l/s inflow through the drain inlet, only 6.4 l/s (32.3 %) and 3.9 l/s (19.7 %) flow were intercepted and drained out by the gully. The flow ratio between manhole inlet and gully pipe plays a significant role in determining the flow circulation pattern inside the manhole.

In this study, the flow path inside the manhole was analysed through the numerical model result. Figure 8 shows different streamline inside the manhole from the above mentioned three simulation results. The yellow streamlines show the flow path coming from the drain and gully whereas the red streamlines are showing the flow path coming through the manhole inlet pipe. The blue arrows show the direction of flow at each case.

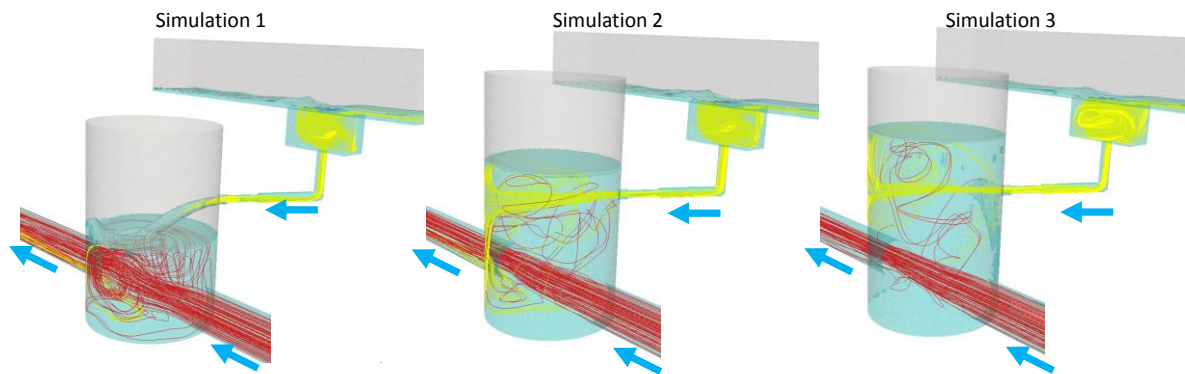


Figure 8: Flow path line / streamline inside the manhole and gully

It can be seen from Figure 8 that both of the flow coming from the gully and manhole inlet circulates inside the manhole and become well mixed. At the left panel, the streamline from simulation 1 shows that the flow from the gully enters the manhole as a plunging jet and recirculates around the manhole. In simulation 1, the flow from the manhole circulates with the manhole. With the increase of surcharge in simulation 2 and 3, the dispersion in manhole inlet flow decreases.

4. CONCLUSION

This study provides first step assessment of flow behaviour inside a gully-manhole linking structure in an urban drainage system. The manhole intakes flow from a gully and adjacent manhole through inlet pipes. A three dimensional CFD model of a quasi-real scale gully-manhole structure was produced using OpenFOAM®, which includes VOF through *interFoam* solver and $k-\epsilon$ turbulence modelling approach. The model shows good agreement with the observed velocity profiles at different plane of the gully.

The flow behaviour at the gully-manhole system was analysed from different surcharge conditions of the manhole. It shows that the intercepted flow by the gully decreases when the surcharge at the manhole. The shear stress at the manhole bottom is much lower than that of gully bottom. This indicates that all the sediment particle sizes transported by the gully will not be transported by this kind of manhole. Some bigger particles may be deposited at the manhole bed. The streamlines from the numerical model showed that the flow from the gully and from manhole inlet becomes well mixed in the manhole. The flow through the manhole inlet showed less depressive nature in higher surcharge.

The study described here is useful to calibrate/validate a numerical model created with the open-source toolbox OpenFOAM® and in characterizing the physical model setup. The work will be further continued to develop an experimental and numerical approach to better understand particulate transport phenomena inside the gully-manhole-pipe drainage. Datasets obtained in this study will be used to calibrate/validate a numerical model created with the open-source toolbox OpenFOAM®.

5. ACKNOWLEDGMENTS

The work presented is part of the QUICS (Quantifying Uncertainty in Integrated Catchment Studies) project. This project has received funding from the European Union's Seventh Framework Programme for research, technological development and demonstration under grant agreement No. 607000. The authors would also like to acknowledge for the support of FCT (Portuguese Foundation for Science and Technology) through the Project UID/MAR/04292/2013 financed by MEC (Portuguese Ministry of Education and Science) and FSE (European Social Fund), under the program POCH (Human Capital Operational Programme).

6. REFERENCES

ANSYS Ins. (2009). *ANSYS Fluent 12.0 User 's Guide*. October.

Beg, M. N. A., Carvalho, R., Lopes, P., Leandro, J., and Melo, N. (2016). "Numerical Investigation of the Flow Field inside a Manhole-Pipe Drainage System." *Hydraulic Structures and Water System Management. 6th IAHR International Symposium on Hydraulic Structures*, B. Crookston and B. Tullis, eds., Portland, Oregon, USA, 1–11.

Brackbill, J. U., Kothe, D. B., and Zemach, C. (1992). "A continuum method for modeling surface tension." *Journal of Computational Physics*, 100(2), 335–354.

Butler, D., and Davies, J. W. (2011). *Urban drainage*. Taylor & Francis, Spon Press, London.

Carvalho, R., Páscoa, P., Leandro, J., Abreu, J., Lopes, P., Quinteiro, R., and Lima, L. M. P. L. (2013). "Experimental investigation of the linking element gully - drop manhole." *Proceedings of 35th IAHR World Congress 2013*, 35th IAHR World Congress 2013.

Djordjević, S., Saul, A. J., Tabor, G. R., Blanksby, J., Galambos, I., Sabtu, N., and Sailor, G. (2013). "Experimental and numerical investigation of interactions between above and below ground drainage systems." *Water Science and Technology*, 67(3), 535–542.

Environmental, B., Commission, I., and Agency, U. S. E. P. (2008). *Simulation of Flow, Sediment Transport, and Sediment Mobility of the Lower Coeur d ' Alene River, Idaho*. U.S. Geological Survey Scientific Investigations Report 2008–5093, Reston, Virginia.

Furbo, E., Harju, J., and Nilsson, H. (2009). *Evaluation of turbulence models for prediction of flow separation at a smooth surface*. Project Report - Uppsala Universitet, Uppsala.

Galambos, I. (2012). "Improved Understanding of Performance of Local Controls Linking the above and below Ground Components of Urban Flood Flows." *PhD Thesis*, University of Exeter.

Greenshields, C. J. (2015). *OpenFOAM User Guide*.

Hirt, C. W., and Nichols, B. D. (1981). "Volume of fluid (VOF) method for the dynamics of free boundaries." *Journal of Computational Physics*, 39(1), 201–225.

Juretić, F. (2015). *cfMesh User Guide (v1.1)*. Zagreb, Croatia.

Leandro, J., Lopes, P., Carvalho, R., Páscoa, P., Martins, R., and Romagnoli, M. (2014). "Numerical and experimental characterization of the 2D vertical average-velocity plane at the center-profile and qualitative air entrainment inside a gully for drainage and reverse flow." *Computers & Fluids*, 102(June), 52–61.

Lopes, P., Leandro, J., Carvalho, R. F., Páscoa, P., and Martins, R. (2015). "Numerical and experimental investigation of a gully under surcharge conditions." *Urban Water Journal*, 12(6), 468–476.

Lopes, P., Leandro, J., Carvalho, R. F., Russo, B., and Gómez, M. (2016). "Assessment of a VOF Model Ability to Reproduce the Efficiency of a Continuous Transverse Gully with Grate." *Journal of Irrigation and Drainage Engineering*, (in production).

Martins, R., Leandro, J., and Carvalho, R. F. (2014). "Characterization of the hydraulic performance of a gully under drainage conditions." *Water science and technology*, 69(12), 2423–30.

Romagnoli, M., Carvalho, R. F., and Leandro, J. (2013). "Turbulence characterization in a gully with reverse flow." *Journal of Hydraulic Engineering-ASCE*, 139(7), 736–744.

Rubinato, M. (2015). "Physical scale modelling of urban flood systems." University of Sheffield.

Rusche, H. (2002). "Computational Fluid Dynamics of Dispersed Two-Phase Flows at High Phase Fractions." *PhD Thesis*, (December).

Stovin, V. R., Guymer, I., and Lau, S. D. (2008). "Approaches to validating a 3D CFD manhole model." *11th International Conference on Urban Drainage (IICUD)*, 1–10.

Weller, H. G. (2002). *Derivation modelling and solution of the conditionally averaged two-phase flow equations. Technical Report TR/HGW/02, Nabla Ltd.*